Sensing and Bio-Sensing Research 27 (2020) 100311

Contents lists available at ScienceDirect

Sensing and Bio-Sensing Research

journal homepage: www.elsevier.com/locate/sbsr

Wide dipole antennas for wireless powering of miniaturised bioelectronic devices

Ammar Aldaoud[a,*], Samuel Lui[b], Kai Sheng Keng[b], Sarina Moshfegh[c], Artemio Soto-Breceda[d,e], Wei Tong[a,e,f], Jean-Michel Redoute[b,g], David J. Garrett[a], Yan T. Wong[b,h], Steven Prawer[a]

[a] School of Physics, University of Melbourne, Parkville, Victoria, Australia
[b] Electrical and Computer Systems Engineering, Monash University, Clayton, Victoria, Australia
[c] School of Biomedical Science, University of Melbourne, Parkville, Victoria, Australia
[d] Department of Biomedical Engineering, University of Melbourne, Parkville, Victoria, Australia
[e] National Vision Research Institute, Australian College of Optometry, Carlton, Victoria, Australia
[f] Department of Optometry and Vision Sciences, University of Melbourne, Parkville, Victoria, Australia
[g] Department of Electrical Engineering and Computer Science, Montefiore Institute, Université de Liège, Liège, Belgium
[h] Department of Physiology and Biomedicine Discovery Institute, Monash University, Clayton, Victoria, Australia

ARTICLE INFO

Keywords:
Wireless power transfer
Bioelectronics
Antennas
Retinal ganglion cells
Injectable
Biological tissue
Finite element method

ABSTRACT

Biomedical electronic implants require a power source to operate. Miniaturised implants can preclude batteries and as implant dimensions reduce further, inductive power transfer no longer becomes the optimum strategy for wireless power delivery. Wide dipole antennas are proposed as an alternative power transmitter for long and thin implants. A miniaturised bioelectronic device measuring 1 mm by 1 mm by 20 mm was fabricated, wirelessly powered and used to stimulate retinal ganglion cells to provide biological validation of its functionality. Optimised wide dipole antennas operating in the GHz range for implant depths of 5 mm to 35 mm in 5 mm steps were simulated, fabricated and measured. Saline solution was used as a biological tissue phantom for power transfer efficiency measurements. The maximum safe deliverable power to the device was 1.7 mW in simulation and 1.3 mW in measurement at power transfer efficiencies of 15% and 11% respectively. The work herein confirms that wide dipole transmitting antennas are suitable for radiative near field power transfer to long and thin implants. This power transfer technique could be used for implants that are injectable, deliverable via catheter and minimally invasive, advancing the aim to create smaller more innovative electronic implantable devices.

1. Introduction

Biomedical microdevices are essential components in the emerging field of therapeutic electrical and optical stimulation. Devices that employ electrical stimulation are already being used to treat Parkinson's disease, depression, epilepsy and rheumatoid arthritis [9]. However, the current generation of stimulating implants tend to be bulky, being comprised of a telemetry unit, cabling and stimulation electrodes [8]. Recent advances by Medtronic and Nanostim have seen the pacemaker shrunk to the size of a large vitamin capsule [4,13]. Hence, there is significant motivation to create biomedical implants that are smaller, less invasive and simpler to surgically implant [6]. Wireless power transfer is a promising technology since it enables miniaturised implants that are small enough to preclude batteries [5].

Typical wireless power transfer schemes to biomedical implants employ inductive coupling. This involves transmitting and receiving coils that are coupled by a time-varying magnetic field (Xue [20]). Although popular, inductive power transfer suffers several limitations as implant size decreases. Kim, Ho & Poon demonstrate that once the receiving coil size is reduced to millimetres in an inductive link the power transfer efficiency drops significantly (2013), and Ma & Poon report that a radiative slotted antenna becomes more efficient [17]. Capacitive coupling can also be advantageous when compared to inductive coupling for some implant geometries. Aldaoud et al. demonstrate the advantages of capacitive coupling for minimally invasive stent-based implants in-vivo [1], reporting on a specific use case for the capacitive coupling regime reported by Jegadeesan et al. [21]. Others report on the advantages of ultrasonic power transfer for miniaturised devices (Vihvelin et al. [22]), while optical wireless power transfer is also presented as another alternative (Ahnood [2]). Inductive coupling remains an effective wireless power transfer regime but it may not be optimal for miniaturised devices or implants that adopt an unusual geometry.

* Corresponding author at: School of Physics, University of Melbourne, Parkville, Victoria, Australia
E-mail address: aaldaoud@student.unimelb.edu.au (A. Aldaoud).

https://doi.org/10.1016/j.sbsr.2019.100311
Received 23 August 2019; Received in revised form 10 November 2019
2214-1804/ Crown Copyright © 2019 Published by Elsevier B.V. This is an open access article under the CC BY-NC-ND license (http://creativecommons.org/licenses/BY-NC-ND/4.0/).

Attempts to shrink biomedical implants to less than one cubic millimetre are reported in the literature but they tend to lack biological validation (Mendes [3]) or not report on the antenna size as part of the device (Chow et al. [22]). The present work shrinks a biomedical implant to be less than a millimetre in two dimensions, creating a string-like device. This morphology is motivated by recent interest in devices that can either be injected or inserted via angiographic catheter [11]. Wireless inductive power transfer is not suitable for a device of these dimensions and a novel wide dipole antenna is created to provide optimum power transfer efficiency in the radiative near-field.

This work extends recent state of the art approaches used to power electric near field dipole antennas implanted in biological tissue. Towe et al. report on the fabrication of a sub-millimetre diameter biomedical device incorporating a small dipole receiver that could provide therapeutic electrical stimulation (2012). Furthermore, Chow et al. report on the design of an intraocular pressure monitor containing a monopole antenna for wireless power and data transfer [22]. Tanabe et al. [15] employ a novel transmitting antenna and report a power transfer efficiency of 10% at a depth of 1 cm for an implanted dipole receiver, suggesting that Towe et al. and Chow et al. could adopt more efficient power transfer regimes (2017). Another possible example includes the commercially available “Freedom Stimulator” from Stimwave that may use a receiving dipole antenna. However, the exact wireless power regime does not appear to have been disclosed. This work demonstrates that a wide dipole transmitting antenna is a suitable alternative to the conformal wireless powering transmitter reported by Tanabe et al. [15]. Moreover, that unlike the conformal wireless power transmitter, the wide dipole transmitter can be optimised in its dimensions and operating frequency to maximise power transfer efficiency for a given implant depth.

This work is split into three sections: section two states the parameters of the wireless power transfer regime being evaluated, section three outlines the simulation and measurement procedures used to determine power transfer efficiency as well as provide biological validation and section four details the results.

2. Problem statement

Consider a half wavelength dipole antenna implanted in biological tissue. Assuming the implant is thin and insulation thickness is small with respect to the conductor diameter, the dipole will resonate at frequency given by,

$$f = \frac{c}{2L\sqrt{\varepsilon_r}}$$

where L is the length of the receiver depicted in Fig. 1a, c is the speed of light in a vacuum and ε_r is the relative permittivity of the biological tissue at the transmission frequency f given a homogenous biological medium. According to Ma & Poon [17], centimetre long implants receive power optimally in the sub-GHz range in biological tissue. In this work L is fixed to 20 mm and by eq. (1), the transmission frequency should be around 1 GHz.

Consider the problem of transmitting power to the implanted dipole antenna. One approach might be to place a transmitting half-wave dipole antenna of length 150 mm above the biological tissue as depicted in Fig. 1a. 150 mm is chosen as it is half a wavelength of 1 GHz in air. A cross section of Fig. 1b is shown in Fig. 1c at a transmission frequency of 1 GHz with the colour map representing the power density. Most of the power in Fig. 1c is lost in the tissue before reaching the implanted dipole.

For an implanted dipole of length L and implant depth D in biological media there must exist an optimum transmitting antenna. The transmitter in Fig. 1a with variable dimensions X and Y and variable transmission frequency f is contrived using the following assumptions. In the first instance ignore the biological media and assume the implanted dipole is electrically very close to the transmitter. It follows that the dominant mode of power transfer is electric near field coupling and the X and Y dimensions should be maximised to increase capacitive coupling between the transmitter and receiver. Now consider the case where the receiving dipole is electrically far from the transmitter. It then follows that an ideal transmitting antenna is in resonance with the receiver. One example of a resonant transmitter is a half-wave dipole antenna. Consider the case where the receiver is somewhere in the order of a wavelength from the transmitter. It follows that a candidate for an optimum transmitting antenna is two plates of dimensions X and Y, meaning the transmitter is somewhere in between the ideal large plate geometry of the electric near field and thin half-wave dipole antenna useful for far field transmission. Therefore, it is proposed that a wide dipole antenna is more suited for transmitting power to an implanted dipole receiver.

Fig. 1d depicts an optimised wide dipole antenna for an implant depth of 10 mm to a receiving dipole 20 mm long with the corresponding power density depicted in Fig. 1e. Compared to the naïve half-wave dipole transmitter in Fig. 1c, the optimised wide dipole antenna has better power transfer efficiency. Hence, there is a wide dipole antenna transmitting at some frequency for a given implant length and depth resulting in optimal power transfer efficiency.

3. Material and methods

First, the simulation procedure used to optimise the wide dipole antenna geometry is detailed. Then, the fabrication process used to create a sub-millimetre diameter receiving device is provided. The device is capable of optical stimulation allowing power transfer efficiency to be measured using a photodiode. Moreover, retinal ganglion cells are optically stimulated by the device wirelessly, validating that it can be used in a biological setting.

3.1. Simulation procedure

Optimum wide dipole antennas for various implant depths were found by performing simulations in CST Microwave Studio®. The receiving implant length was fixed to 20 mm and an arbitrary implant diameter of 0.1 mm was chosen. Implant depths from 1 mm to 40 mm in 1 mm steps were considered and muscle was used as approximate average biological medium (Ma & Poon [17]). For each implant depth D, simulations using a parametric sweep of X and Y, the wide dipole antenna arm length and width were performed from 1 mm to 40 mm in 1 mm steps. Simulations were performed using a finite difference time domain (FDTD) method for frequencies in the range of 0.5 to 1.5 GHz. Hence, the optimisation strategy can be summarised as follows: for a given implant depth D, there exists some tuple (X,Y,f) resulting in a maximum power transfer efficiency to the receiving dipole implanted in biological media. Optimum tuple values are depicted in Fig. 4a, b and c.

Once the optimum tuple (X,Y,f) was calculated for each implant depth D, several other parameters were determined. A measure of deleterious tissue heating called the specific absorption rate (SAR) was calculated by first fixing the transmitting antenna source to 1 V and its optimum transmission frequency f. The 1 g averaged SAR was then recorded. To find the maximum input power, the input power at the transmitter was increased until the SAR safety limit of 1.6 W/kg averaged over 1 g of tissue was reached (IEEE std. [15]). The power at the receiving dipole was recorded and taken to be the maximum output power of the wireless link. The steps above were repeated for a multilayer tissue model with 2 mm of skin and 5 mm of fat above the muscle volume. Implant depths of 10 mm to 40 mm in 1 mm steps, instead of 1 mm to 40 mm, were chosen to avoid the receiving implant being surround by skin or fat, ensuring comparable results between the homogenous and multilayer tissue models. The steps above were also repeated, except for the optimisation stage, for a half-wave dipole transmitter with homogenous muscle tissue as well as with a multilayer tissue model. The results comparing the half-wave dipole transmitter to

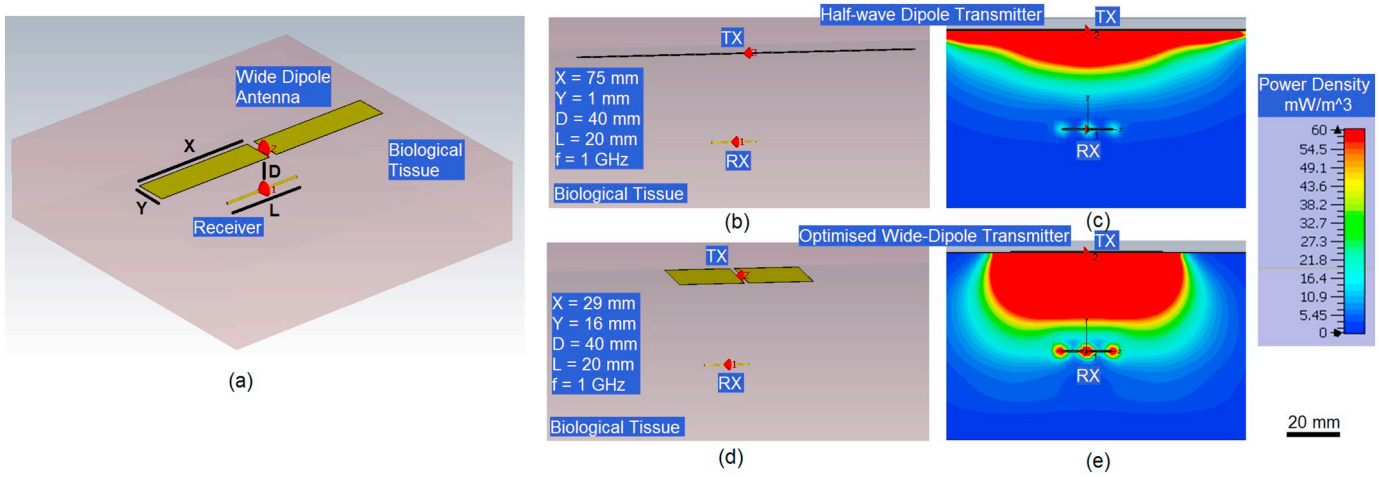

Fig. 1. Finite element simulation demonstrating that optimised wide dipole antennas are more efficient than a classical half wave dipole antenna. (a) Variable parameters in a wide dipole power transfer regime: plate dimensions X and Y, implant depth D and implant length L (b) Design example employing a classical half wave dipole antenna (c) corresponding power density in simulation for half wave dipole (d) Design example employing an optimised wide dipole antenna (e) corresponding power density in simulation for an optimised wide dipole antenna. The optimised geometry in (d) has greater power transfer efficiency than the classical geometry in (b).

the optimised wide dipole transmitter in muscle and a multilayer tissue model are summarised in Fig. 4.

3.2. Device fabrication

A sub-millimetre diameter device, 20 mm long that is capable of receiving wireless RF power and outputting optical power was fabricated. Bare surface mount devices were soldered together directly to avoid the need for a printed circuit board to minimise device size. The electronic schematic is depicted in Fig. 2a. Two, 1 cm long, 100 µm diameter copper wire lengths form the dipole receiving antenna. The incoming AC signal from the antenna is converted to DC using a zero-bias voltage doubling rectifier made from two capacitors and two diodes. Two 100 pF 0201 sized (600 µm by 300 µm by 300 µm) capacitors with NP0 dielectric were chosen due to their small size and suitable RF properties. The diodes are 0201 sized RF Schottky diodes that were chosen due to their low forward voltage drop and junction capacitance. A low power 0402 sized LED was connected to the output of the rectifier to provide optical stimulation to target cells. The device was coated in PDMS to avoid toxic materials contacting cells during biological validation. A complete fabricated device is depicted in Fig. 2c along with a sugar grain for size comparison.

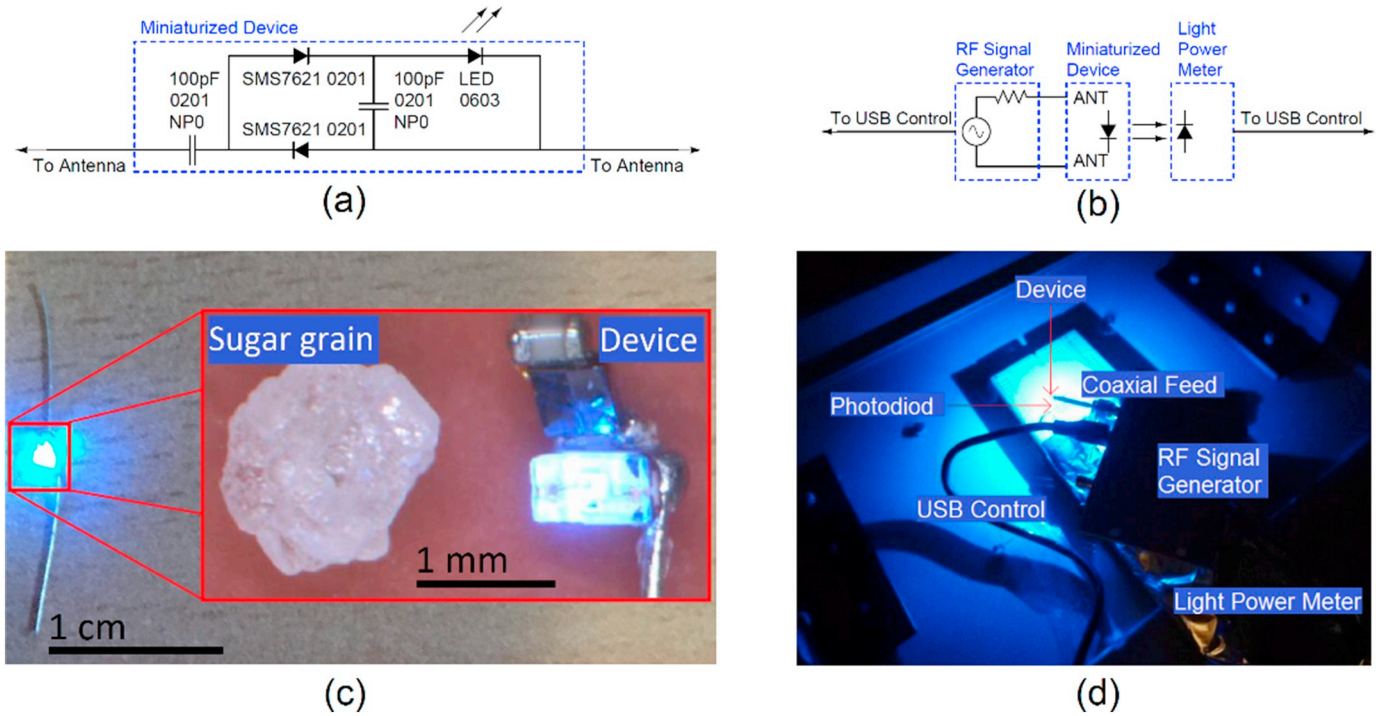

Fig. 2. (a) Electronic schematic for miniaturised submillimeter diameter receiving device with a voltage doubling rectifier powering an LED (b) Fabricated submillimeter diameter device with components soldered directly together to minimise size (c) Electronic schematic of calibration set up used to determine light output power of device given a known power and frequency at input (d) Depiction of experimental calibration set up.

3.3. Calibration procedure

The fabricated device in Section 3.2 can be used for power transfer efficiency measurements to verify the simulations in Section 3.1. Before this can be done the efficiency of the implant itself must be determined. That is, how efficiently the received RF power at the antenna is converted to optical power. This later permits the calculation of the power transfer efficiency of the wireless link by measuring the optical output power. The receiving device was placed and glued to a transparent container and the 1 cm long antenna lengths were removed. An RF signal generator was connected directly to the device via a short coaxial cable. A custom light power meter made from a photodiode and microcontroller development board was used to measure the light intensity. A constant input power of 5 dBm from the RF signal generator was set and the ADC values from the light power meter were recorded for RF frequencies of 0.5–1.5 GHz.

3.4. Power transfer efficiency measurement procedure

A typical power transfer efficiency measurement set up would involve a coaxial cable connected to the receiver. However, due to the receiver size the coaxial cable would add a significant amount of ground to the device, artificially increasing the amount of power received. Instead, a novel power transfer efficiency measurement scheme is employed where the optical output power is measured. This electrically isolates the receiving device from the measurement instrument. The procedure is described as follows with the complete set up depicted in Fig. 3. A USB controlled RF signal generator was connected to an RF amplifier. Seven different wide dipole antennas were fabricated on FR4 for implant depths of 5 mm to 35 mm in 5 mm steps. The dimensions *X and* Y of the optimal wide dipole antenna for a given depth and optimal operating frequency *f* were determined by the simulations in Section 3.1 and are shown in Fig. 4a and c. Furthermore, each wide dipole antenna had a corresponding 1:1 balun soldered to it to ensure the unbalanced coaxial feed from the antenna was suitably matched to the balanced feed required for the wide dipole antenna. A 1:1 balun along with a wide dipole antenna is depicted in Fig. 3b and the dimensions *a* and *b* depend on the operating frequency of the antenna such that *a* is a quarter wavelength and *b* is three quarters of a wavelength.

The same custom light power meter from Section 3.3 was used to measure the light output power of the device glued to the base of the transparent container. A Perspex fixture was fabricated to adjust the transmitting antenna distance from the receiving device, effectively adjusting the implant depth. Perspex was chosen since metallic materials could interfere with the power transfer efficiency measurements. The transparent container was filled with 0.5% saline solution to emulate biological tissue (Ma & Poon [17]). The solution was adjusted in depth from 5 mm to 35 mm in 5 mm steps and the wide dipole antenna and balun were replaced for each implant depth. The antenna was then driven at its optimum frequency. The output power of the RF signal generator was adjusted until the light power meter reached an ADC value corresponding to 5 dBm of received power at the device input. The power transfer efficiency of the radiative near field link was then calculated.

3.5. Biological validation

Biological validation was performed using the set up depicted in Fig. 5b. The current-clamp technique described previously Soto-Breceda et al. [12], Aldaoud et al, [1] was used to obtain whole cell recordings of a retinal ganglion cell. In brief, an adult rat was anaesthetized with a mixture of Ketamine (100 mg/kg) and Xylazine(10 mg/kg) and then killed. The retina was then dissected, flat-mounted with the retinal ganglion cells side up on a glass coverslip. To obtain a whole

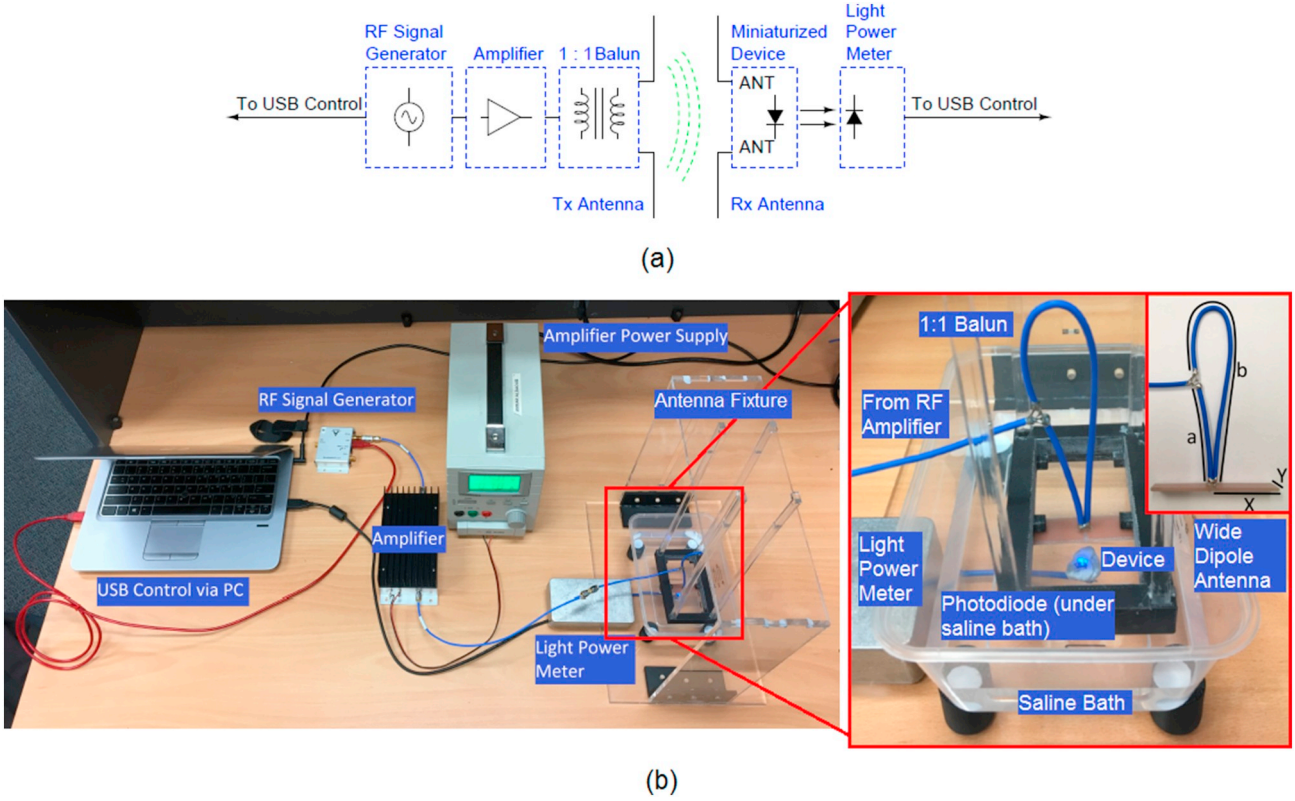

Fig. 3. (a) Schematic of set up used to determine power transfer efficiency for a given implant depth in 0.5% saline solution. A USB controlled RF signal generator feeds a power amplifier which feeds a balun, powering an optimised wide dipole antenna for the given implant depth. A light power meter detects the device output power so that power transfer efficiency can be calculated (b) depiction of experimental set up explained in (a).

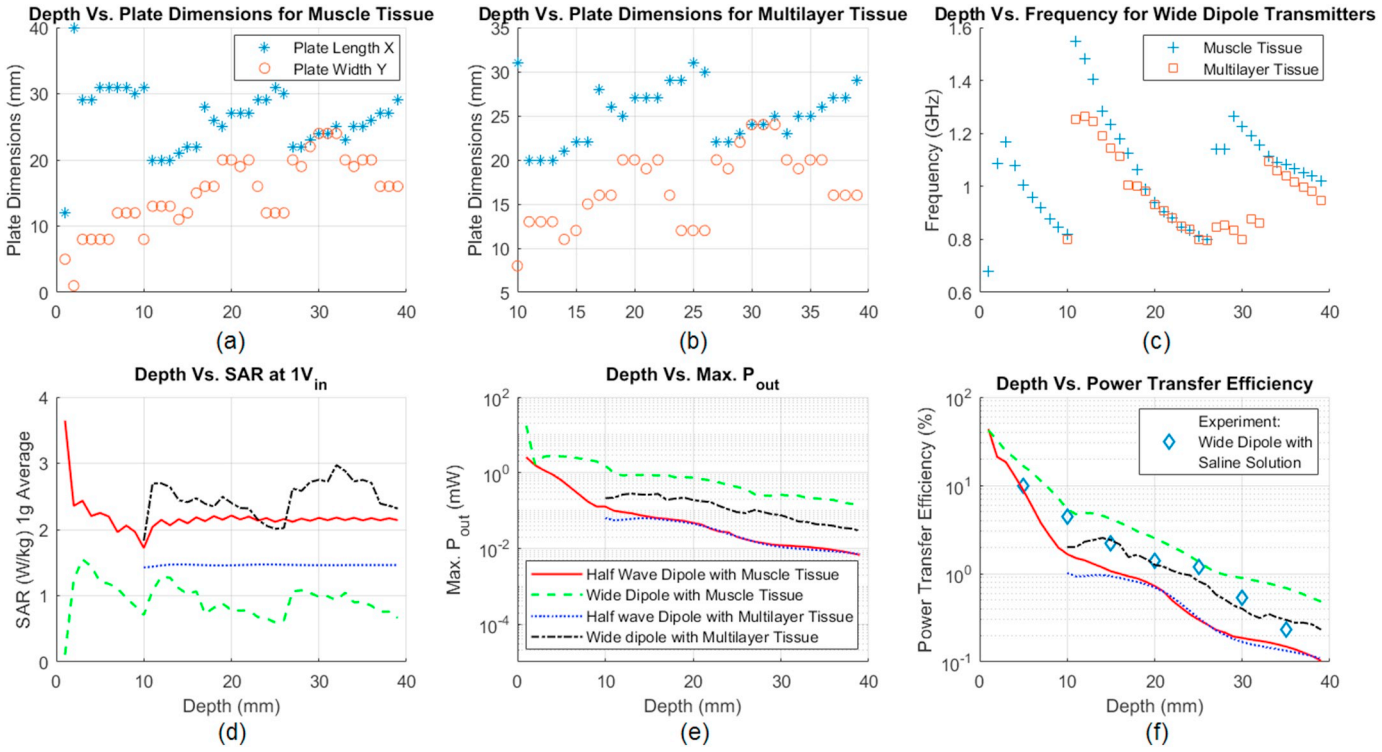

Fig. 4. Simulation and measurement results for the radiative wireless power transfer regime described in this work (a) Optimised wide dipole antenna dimensions for maximum power transfer efficiency vs implant depth in muscle tissue (b) Optimised wide dipole antenna dimensions for maximum power transfer efficiency vs implant depth in a multilayer tissue model (2 mm skin, 5 mm fat, muscle) (c) Optimum transmission frequency for maximum power transfer efficiency vs implant depth for optimised wide dipole antennas (d) Simulation results for specific absorption rate vs implant depth for traditional half wave dipole antennas and optimised wide dipole antennas with muscle tissue and a multilayer tissue model (e) Simulation results for maximum power available at receiver vs implant depth for traditional half wave dipole antennas and optimised wide dipole antennas with muscle and a multilayer tissue model (f) Power transfer efficiency vs implant depth in simulation and experiment.

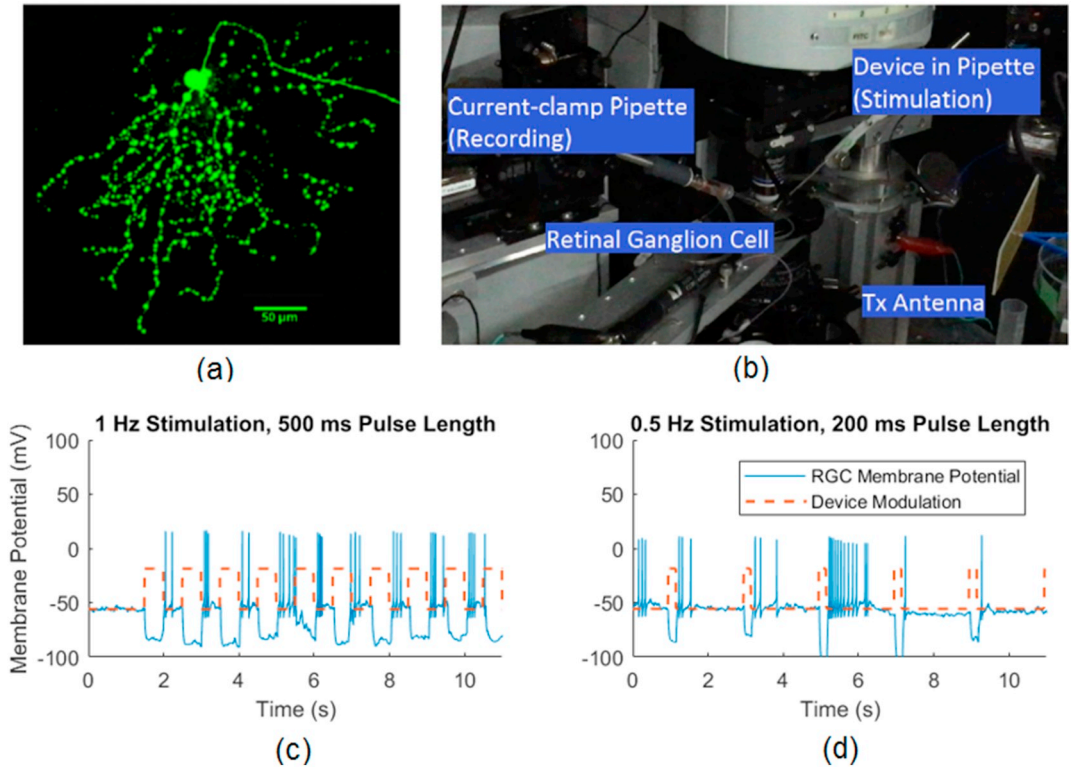

Fig. 5. Test setup and results for device biological validation (a) Retinal ganglion cell (b) patch clamp set up with device placed inside pipette and above cell (c) retinal ganglion cell response to 1 Hz modulation with a 500 ms pulse length (d) retinal ganglion cell response to 0.5 Hz stimulation with a 200 ms pulse length. The cell in (a) is therefore an OFF type.

cell recording a sharp glass pipette was used to make a hole in the inner limiting membrane of a retinal ganglion cell to expose the cell to be tested. The cell was then patch-clamped with a recording glass pipette. The RF transmitter was then driven at 1 GHz, 1 Hz modulation, 50% duty cycle and 1 GHz, 0.5 Hz modulation, 20% duty cycle without the device present to ensure the retinal ganglion cell did not respond to the 1 GHz RF signal. The stimulating device was then placed in a pipette above the glass coverslip and the RF transmitter was driven again. The retinal ganglion cell response to the optical stimulation was recorded. The recorded retinal ganglion cell was imaged with a confocal microscope and the morphology was reconstructed with depth imaging. The intracellular solution that fills the recording pipette includes Alexa Fluor 488 (fluorescent) dye, which fills the retinal ganglion cell during recording, hence one can see the morphology of the retinal ganglion cell under bright light after the experiment as shown in Fig. 5a. All animal experiments were conducted as per the policies of National Health and Medical Research Council of Australia and were approved by the Animal Ethics Committee of the University of Melbourne.

4. Results

4.1. Power transfer simulations

The power transfer simulations in Section 3.1 yield the results depicted in Fig. 4. Fig. 4a, b and c show the optimum dimensions, X and Y and optimum frequency f for wide dipole antennas powering a receiving dipole of length 20 mm implanted at a depth D in muscle tissue as well as in a multilayer tissue model. The multilayer tissue model is 2 mm of skin, 5 mm of fat and then muscle. Quantities a and b in the insert in Fig. 3b are calculated using the transmission frequency f and are the dimensions for the 1:1 balun connected to the wide dipole antenna. The optimum dimensions for a wide dipole antenna that transmits with the highest efficiency differ depending on the biological medium. Fig. 4a shows the optimum dimensions for muscle whereas Fig. 4b is for a multilayer tissue model, which includes skin and fat as well as muscle. The optimum transmission frequencies for muscle and a multilayer tissue model show a similar trend. Therefore, even with a changing biological medium the optimum frequency remains similar. However, if this wireless power transfer method were to be adopted in a clinical setting the transmitting antenna would need to be optimised in dimension depending on the location of the implant and the surrounding biological material.

The optimised wide dipole antenna outperforms the traditional half wave dipole antenna in maximum output power and power transfer efficiency. Fig. 4e and f demonstrate that the advantages of using an optimised wide dipole antenna are more pronounced in muscle than in a multilayer tissue model. The simulations were performed from depths of 10 mm to 40 mm in the multilayer tissue model to ensure the receiving dipole would consistently be surrounded by muscle due to the 2 mm of skin and 5 mm of fat above the muscle tissue. The specific absorption rate (SAR) results for muscle differ notably from the multilayer tissue model. The SAR measure determines the maximum input power to the transmitter as a SAR of 1.6 W/kg is generally considered the safety threshold (IEEE std. [15]). When the biological medium is homogenous muscle tissue, the wide dipole antenna results in lower SAR than the half wave dipole antenna. However, the multilayer tissue model responds in the opposite way with the half wave dipole causing less tissue heating. SAR safety thresholds limit how much power can be provided at the input of the transmitter. However, the wide dipole antenna transmission efficiency overcomes the limitations of the SAR safety threshold meaning the maximum output power for a multilayer tissue model with wide dipole transmitter is still greater than that of a multilayer tissue model with a halfwave dipole antenna. The depth vs. optimum transmission frequency shows some pattern with singularities appearing at 10 mm and 30 mm whereas the depth vs. optimum antenna dimensions does not appear to follow a pattern. This is likely due to the non-linear and dispersive nature of electromagnetic waves interacting with biological tissue.

4.2. Power transfer measurements

Fig. 4f depicts a comparison between the power transfer efficiency simulation results from Section 3.1 and the measurement results from Section 3.4. The 0.5% saline solution is intended to emulate the electrical properties of muscle tissue. However, it can be observed that the measurement results are closer to the multilayer tissue simulation model. There are many possible reasons for the slight discrepancy between the simulation and measurement results. The RF signal generator used has a 0.5 dB output amplitude step size, the RF amplifier does not have a flat frequency vs output power response and saline solution is not a perfect model of biological tissue. Whether the optimum frequency in simulation is also the optimum frequency in measurement is difficult to determine. Since the wide dipole antenna has a narrow bandwidth 1:1 balun attached, a frequency sweep in measurement would not be comparable to the simulation results. Nevertheless, the measurement results do follow a similar trend to the simulation results.

Although the experimental set up is effective in obtaining measurement results, it does have drawbacks. It is tedious to glue the implant at the bottom of the transparent container, glue the photodiode in place, remove the receiving antenna from the device, power the device directly from the signal generator to obtain calibration readings and then reattach the antenna to the device, while keeping it in the exact same position and not damaging it. If the position of the device changes, the amount of light detected by the photodiode also changes and the measurement results become inaccurate. The measurement method is also limited as it relies on the use of a transparent medium to permit the light to transmit power to the photodiode. In this instance, saline solution is used but it would be desirable to use porcine tissue or blood as these biological media might provide more meaningful measurement results. Ma & Poon report the use of a fibre optic cable coupled to their device's LED for received power measurements [17]. However, this adds further complexity as the loss at the input to the fibre optic cable and the output from the cable to the sensor needs to be considered. Ma & Poon report a similar discrepancy between simulation and measurement results in saline solution [17].

4.3. Biological validation

The retinal ganglion cell response to optical stimulation from the device is depicted in Fig. 5c and d. It can be observed that the retinal ganglion cell membrane potential is affected by the wirelessly modulated light source as the cell shows spiking activity in response to the light source. Two different stimulation regimes with different modulation frequency and pulse length provide further confirmation. The cell is an OFF type, since the membrane potential drops when the light is on and spikes are only observed after the light is switched off. It is worth noting that the transmission medium used for the biological experiment is air, whereas the power transfer efficiency experiments used saline solution. Air attenuates the transmitted power to the device less than biological material, so the biological validation experiment is not comparable with the power transfer efficiency experiment and the light output power of the LED is not known. The interesting aspect of the biological experiment is that the device is placed within a narrow pipette as shown in Fig. 5b, supporting the possibility of the device being used for delivery via injection or catheter. Furthermore, the biological experiment was also performed with the transmitting antenna turned on, without the device present. The retinal ganglion cell did not respond to the GHz frequency signals used to power the device, demonstrating that the wireless power transfer regime described in this work did not unintentionally cause a physiological cell response.

Table 1
Comparison of the work herein to the state of the art. By extending the receiving device size in only one dimension the power transfer efficiency is increased by one or two orders of magnitude when compared to other radiative power transfer regimes. In at least one case, the power transfer efficiency of this work exceeds that of a large sized receive using an inductive power transfer regime. All comparative works use biological tissue or a suitable phantom as the transmission medium with two exceptions: *transmission medium is 1 cm chicken breast and 1 cm air **exact distance between transmitter and receiver is unclear but must be at least 2.5 mm.

Reference	Wireless Method	Power Transfer Efficiency	Device Dimensions
This work	Radiative	5% at 10 mm	20 mm by < 1 mm by < 1 mm
Tanabe [15]	Radiative	10% at 10 mm	13 mm by 2 mm by 1 mm
Biswas [16]	Inductive	1.4% at 5 mm	11.25 mm by 6 mm by 1.57 mm
Ma [17]	Radiative	0.075% at 10 mm	2 mm by 2 mm by 2 mm
Rahmani [18]	Radiative	0.23% at 20 mm*	1.6 mm by 1.6 mm by < 1 mm
Ding [19]	Radiative	0.0014% at 10 mm	10 mm by 10 mm by 1 mm
Anacleto [3]	Radiative	0.5%**	0.5 mm by 0.5 mm by 0.5 mm

5. Discussion

It is difficult to verify the optimum operating frequency and antenna dimensions for a given depth in measurement. Verifying the frequency would be challenging since the 1:1 balun has a narrow bandwidth. A wide bandwidth 1:1 balun would need to be designed, fabricated, tested and measured. Verifying the optimum antenna dimensions found through simulation presents an even greater challenge. Since the parametric sweep for the *X* and *Y* dimensions covers 1 mm to 40 mm in 1 mm steps, this would involve fabricating 1600 different antennas. Nevertheless, the measurements provide enough verification to demonstrate that antenna dimensions and operating frequency can be optimised for implant depth. Since the receiving implant is within the radiative near field of the transmitting antenna, it is expected that the receiver can influence the transmitter characteristics [14].

The custom antenna dimensions based on implant depth presents pros and cons. By customising the antenna, power transfer efficiency is increased, increasing the amount of available power at the receiving device. However, system complexity and implementation are also a consideration and a design that uses custom antennas based on implant depth may not be suitable for all bioelectronic applications. It should be mentioned that electric dipoles are generally much less efficient than magnetic dipoles for implantable devices, due to the absorption incurred by the predominantly electric reactive field. A comparison is provided by Nikolayev et al. [10].

The results in this work demonstrate that wide dipole antennas are a promising option for wireless power transfer to sub-millimetre diameter devices. Several avenues exist by which this work could be extended. The wide dipole antennas that were fabricated are rigid and the simulations also assumed a rigid antenna. If the antenna is to be worn on a subject, a flexible wide dipole antenna would be more functional for the user (Agrawal 2017). Exploring how a flexible wide dipole antenna interacts with biological tissue would require further extensive simulations. Moreover, there is no obvious measurement strategy for determining the power transfer efficiency of a flexible wide dipole antenna. This work also assumes that the transmitting antenna is positioned above the receiving device. Future opportunities also include determining the influence of transmitting antenna offset and angular displacement.

The measurement results for power transfer efficiency differ from the simulation results marginally in Fig. 4f. Many possible sources of error exist, particularly since the set up in Fig. 3 is complex. Possible sources of error include the RF output power of the signal generator, the gain of the RF amplifier, losses in the coaxial cables, inaccuracies in the use of saline solution as a biological tissue model, ambient light sources, photodiode displacement and ADC error from the light power meter. A simpler set up to measure power transfer efficiency would include a coaxial cable connected directly to the receiving device. However, due to the extremely small size of the receiving device, any length of coaxial cable or electrically connected instrumentation adds extra grounding. Artificially and significantly increasing the received power. Given the complexity of the experimental set up, the error seen when comparing simulation and measurement results can be considered reasonable.

Table 1 provides comparison between this work and the current state of the art. Tanabe et al. reports the highest power transfer efficiency of 10% at an implant depth of 10 mm for a similarly sized device (2017). However, Tanabe et al. [15] also report a power transfer efficiency of < 1% at 20 mm, which is surpassed experimentally in this work (2017). The other devices reported in the literature report power transfer efficiencies one or two orders of magnitude less than what is reported in this work. However, they tend to aim to be small in all three dimensions. Therefore, significant gains in power transfer efficiency can be made by increasing the size of an implanted device in only a single dimension.

6. Conclusion

This work details the simulation, design, fabrication and measurement of a miniaturised bioelectronic device measuring 1 mm by 1 mm by 20 mm. By optimising the transmitting wide dipole antenna dimensions and operating frequency, it is possible to improve power transfer efficiency. To the authors' knowledge this work is the first to demonstrate that wide dipole antennas can be optimised to transmit power to a sub-millimetre diameter biomedical implants. Furthermore, submillimetre diameter devices show potential to be injectable as demonstrated by placing the device into the end of a pipette and stimulating retinal ganglion cells. This work advances the state of the art in creating smaller more innovative electronic implantable devices.

Declaration of Competing Interests

The authors declare that they have no known competing financial interests or personal relationships that could have appeared to influence the work reported in this paper.

Acknowledgements

The authors would like to thank the anonymous reviewers for their helpful comments and contributions. This work was funded by the National Health and Medical Research Council (NHMRC) of Australia, grant GNT1101717.

References

[1] A. Aldaoud, A. Soto-Breceda, W. Tong, G. Conductier, M.A. Tonta, H.A. Coleman, ... S. Prawer, Wireless multichannel optogenetic stimulators enabled by narrow bandwidth resonant tank circuits, Sensors & Actuators: A. Physical 271 (2018) 201–211, https://doi.org/10.1016/j.sna.2017.12.051.
[2] A. Ahnood, K.e. Fox, N.v. Apollo, A. Lohrmann, D.j. Garrett, D.a.a. Nayagam, ... S. Prawer, Diamond encapsulated photovoltaics for transdermal power delivery, Biosens. Bioelect. 77 (2016) 589–597, https://doi.org/10.1016/j.bios.2015.10.022.
[3] P.A.M. Anacleto, Self-Folding 3D Micro Antennas for Implantable Medical Devices, (2016), https://doi.org/10.1142/S2339547816500047.
[4] M.F. El-Chami, F. Al-Samadi, N. Clementy, C. Garweg, J.L. Martinez-Sande,

J.P. Piccini, ... P.R. Roberts, Updated performance of the Micra transcatheter pacemaker in the real-world setting: a comparison to the investigational study and a transvenous historical control, Heart Rhythm. 15 (12) (2018) 1800–1807, https://doi.org/10.1016/j.hrthm.2018.08.005.

[5] B. Ghafari, Ultra-Low Power, Low-Noise and Small Size Transceiver for Wearable and Implantable Biomedical Devices and Neural Prosthesis, (2019).

[6] C.A. Giller, P. Jenkins, Some technical nuances for deep brain stimulator implantation, Interdisc. Neurosurg. Adv. Tech. Case Manage. 2 (1) (2015) 29–39, https://doi.org/10.1016/j.inat.2014.11.001.

[7] IEEE Recommended Practice for Determining the Peak Spatial-Average Specific Absorption Rate (SAR) in the Human Head from Wireless Communications Devices: Measurement Techniques - Redline, IEEE Std 1528-2013 (Revision of IEEE Std 1528–2003) - Redline, (2013), p. 1.

[8] Kimura Takehiro, Miyoshi Shunichiro, Okamoto Kazuma, Fukumoto Kotaro, Tanimoto Kojiro, Soejima Kyoko, ... Fukuda Keiichi, The effectiveness of rigid pericardial endoscopy for minimally invasive minor surgeries: cell transplantation, epicardial pacemaker lead implantation, and epicardial ablation, J. Cardiothorac. Surg. (1) (2012) 117, , https://doi.org/10.1186/1749-8090-7-117.

[9] A. Majid, Electroceuticals: advances in electrostimulation therapies, Springer. (UniM INTERNET resource). (2017) 1–33 https://www.springer.com/gp/book/9783319286105.

[10] D. Nikolayev, M. Zhadobov, P. Karban, R. Sauleau, Electromagnetic radiation efficiency of body-implanted devices, Phys. Rev. Appl. 9 (2) (2018), https://doi.org/10.1103/PhysRevApplied.9.024033.

[11] J. Park, J.-K. Kim, S.A. Park, D.-W. Lee, Biodegradable polymer material based smart stent: wireless pressure sensor and 3D printed stent, Microelectron. Eng. 206 (2019) 1–5, https://doi.org/10.1016/j.mee.2018.12.007.

[12] A. Soto-Breceda, T. Kameneva, H. Meffin, M. Maturana, M.R. Ibbotson, Irregularly timed electrical pulse reduce adaptation of retinal ganglion cells, J. Neural Eng. 15 (5) (2018), https://doi.org/10.1088/1741-2552/aad46e.

[13] J. Sperzel, C. Hamm, A. Hain, Nanostim-leadless pacemaker, Herzschrittmacherther. Elektrophysiol. 29 (4) (2018) 327–333, https://doi.org/10.1007/s00399-018-0598-3.

[14] G. Stockman, H. Rogier, D.V. Ginste, Dedicated model for the efficient assessment of wireless power transfer in the radiative near-field, Int. J. Numer. Model. 29 (3) (2016) 380–391, https://doi.org/10.1002/jnm.2075.

[15] Y. Tanabe, J.S. Ho, J. Liu, S.-Y. Liao, Z. Zhen, S. Hsu, ... A.S.Y. Poon, High-performance wireless powering for peripheral nerve neuromodulation systems, PLoS One 12 (10) (2017) 1–13, https://doi.org/10.1371/journal.pone.0186698.

[16] Dipon K. Biswas, Melissa Sinclair, Joshua Hyde, Ifana Mahbub, An NFC (near-field communication) based wireless power transfer system design with miniaturized receiver coil for optogenetic implants, 2018 Texas Symposium on Wireless and Microwave Circuits and Systems (WMCS), Wireless and Microwave Circuits and Systems (WMCS), 2018 Texas Symposium On, 1, (2018), https://doi.org/10.1109/WMCaS.2018.8400620.

[17] A. Ma, A.S.Y. Poon, Midfield Wireless Power Transfer for Bioelectronics, IEEE Circuits and Systems Magazine, Circuits and Systems Magazine, IEEE, IEEE Circuits Syst. Mag 2 (2015) 54, https://doi.org/10.1109/MCAS.2015.2418999.

[18] Hamed Rahmani, Aydin Babakhani, A wireless power receiver with an on-chip antenna for millimeter-size biomedical implants in 180 nm SOI CMOS, 2017 IEEE MTT-S International Microwave Symposium (IMS), Microwave Symposium (IMS), 2017 IEEE MTT-S International, 2017, p. 300, , https://doi.org/10.1109/MWSYM.2017.8059103.

[19] Shuoliang Ding, Stavros Koulouridis, Lionel Pichon, A Dual-Band Miniaturized Circular Antenna for Deep in Body Biomedical Wireless Applications, 2019 13th European Conference on Antennas and Propagation (EuCAP), Antennas and Propagation (EuCAP), 2019 13th European Conference On, 1, 2019, https://doi.org/10.1109/MWSYM.2017.8059103 https://search-ebscohost-com.ezp.lib.unimelb.edu.au/login.aspx?direct=true&db=edseee&AN=edseee.8739829&site=eds-live&scope=site Retrieved from.

[20] Xue Rui-Feng, Cheng Kuang-Wei, Je Minkyu, High-Efficiency Wireless Power Transfer for Biomedical Implants by Optimal Resonant Load Transformation, IEEE Transactions on Circuits and Systems I: Regular Papers, Circuits and Systems I: Regular Papers, IEEE Transactions on, IEEE Trans. Circuits Syst. I 4 (2013) 867, https://doi.org/10.1109/TCSI.2012.2209297.

[21] R. Jegadeesan, Xin Guo Yong, Je Minkyu, Electric near-field coupling for wireless power transfer in biomedical applications, 2013 IEEE MTT-S International Microwave Workshop Series on RF and Wireless Technologies for Biomedical and Healthcare Applications (IMWS-BIO), Microwave Workshop Series on RF and Wireless Technologies for Biomedical and Healthcare Applications (IMWS-BIO), 2013 IEEE MTT-S International, 1, 2013, https://doi.org/10.1109/IMWS-BIO.2013.6756140.

[22] H. Vihvelin, J. Leadbetter, M. Bance, J.A. Brown, R.B. Adamson, Compensating for Tissue Changes in an Ultrasonic Power Link for Implanted Medical Devices, IEEE TRANSACTIONS ON BIOMEDICAL CIRCUITS AND SYSTEMS 2 (2016) 404 https://search-ebscohost-com.ezp.lib.unimelb.edu.au/login.aspx?direct=true&db=edsbl&AN=RN376815700&site=eds-live&scope=site Retrieved from.

[22] E.Y. Chow, S. Chakraborty, W.J. Chappell, P.P. Irazoqui, Mixed-signal integrated circuits for self-contained sub-cubic millimeter biomedical implants, 2010 IEEE International Solid-State Circuits Conference - (ISSCC), (2010), pp. 236–237, https://doi.org/10.1109/ISSCC.2010.5433933 http://ieeexplore.ieee.org/stamp/stamp.jsp?tp=&arnumber=5433933&isnumber=5433812 San Francisco, CA.